Predictive and Therapeutic Implications of a Novel PLCγ1/SHP2-Driven Mechanism of Cetuximab Resistance in Metastatic Colorectal Cancer

Raquel Cruz-Duarte[1], Cátia Rebelo de Almeida[2], Magda Negrão[2], Afonso Fernandes[1], Paula Borralho[3], Daniel Sobral[4], Lina M. Gallego-Paez[5], Daniel Machado[6], João Gramaça[6], José Vílchez[6], Ana T. Xavier[6], Miguel Godinho Ferreira[2,7], Ana R. Miranda[8], Helder Mansinho[8], Maria J. Brito[9], Teresa R. Pacheco[1,10], Catarina Abreu[10], Ana Lucia-Costa[10], André Mansinho[1,10], Rita Fior[2], Luís Costa[1,10], and Marta Martins[1]

ABSTRACT

Purpose: Cetuximab is an EGFR-targeted therapy approved for the treatment of *RAS* wild-type (WT) metastatic colorectal cancer (mCRC). However, about 60% of these patients show innate resistance to cetuximab. To increase cetuximab efficacy, it is crucial to successfully identify responder patients, as well as to develop new therapeutic approaches to overcome cetuximab resistance.

Experimental Design: We evaluated the value of EGFR effector phospholipase C gamma 1 (PLCγ1) in predicting cetuximab responses, by analyzing progression-free survival (PFS) of a multicentric retrospective cohort of 94 treated patients with mCRC (log-rank test and Cox regression model). Furthermore, we used *in vitro* and zebrafish xenotransplant models to identify and target the mechanism behind PLCγ1-mediated resistance to cetuximab.

Results: In this study, levels of PLCγ1 were found increased in *RAS* WT tumors and were able to predict cetuximab responses in clinical samples and *in vitro* and *in vivo* models. Mechanistically, PLCγ1 expression was found to bypass cetuximab-dependent EGFR inhibition by activating ERK and AKT pathways. This novel resistance mechanism involves a noncatalytic role of PLCγ1 SH2 tandem domains in the propagation of downstream signaling via SH2-containing protein tyrosine phosphatase 2 (SHP2). Accordingly, SHP2 inhibition sensitizes PLCγ1-resistant cells to cetuximab.

Conclusions: Our discoveries reveal the potential of PLCγ1 as a predictive biomarker for cetuximab responses and suggest an alternative therapeutic approach to circumvent PLCγ1-mediated resistance to cetuximab in patients with *RAS* WT mCRC. In this way, this work contributes to the development of novel strategies in the medical management and treatment of patients with mCRC.

Introduction

Colorectal cancer is the third most common cancer worldwide and the second leading cause of cancer-related death (1). The high mortality of patients with colorectal cancer is mainly due to the metastatic spreading. EGFR is a growth factor receptor frequently deregulated in colorectal cancer (60%–80% of cases), which plays a key role in tumor development and progression (2). Accordingly, EGFR-targeted therapies are associated with survival benefit of patients with mCRC and represent nowadays a valuable option for the treatment of this disease (3, 4).

Cetuximab is a human–mouse chimeric mAb that binds to EGFR, blocks its ligand-binding activation causing receptor internalization and degradation, which inhibits the full signaling cascade transmission (5). In addition, cetuximab induces antibody-mediated cytotoxicity due to its ability to elicit an immune response by the innate (macrophages and dendritic cells) and the adaptive ($CD8^+$ T and NK cells) immune system (6, 7).

Unfortunately, only a small subset of patients with mCRC respond to cetuximab. In unselected patients, cetuximab treatment, in combination with chemotherapy-based regimes (FOLFIRI/FOLFOX), is associated with only 10% of objective response rates (ORR; refs. 8, 9). Therapy efficacy increases to around 36% when the same combinatorial treatment is administered to *KRAS* and *NRAS* (hereafter designed by *RAS*) WT patients (8, 9). Thus, cetuximab was shown to be contraindicated in *RAS* mutant tumors, given their constitutive activation of downstream signaling, which renders EGFR-directed therapies ineffective. Indeed, *RAS* mutational status is currently the only clinically approved predictive biomarker of lack of response to anti-EGFR therapies in patients with mCRC. Following the same rational, activating mutations on other EGFR downstream effectors, such as *BRAF* and *PIK3CA*, were also recognized mechanisms of resistance to cetuximab, resulting in ORRs of about 42% in *KRAS*/

[1]Instituto de Medicina Molecular- João Lobo Antunes, Faculdade de Medicina, Universidade de Lisboa, Lisbon, Portugal. [2]Champalimaud Centre for the Unknown, Champalimaud Foundation, Lisbon, Portugal. [3]Institute of Pathology, Faculdade de Medicina, Universidade de Lisboa, Lisbon, Portugal. [4]Universidade Nova Lisboa, UCIBIO, Departamento de Ciências da Vida, Faculdade de Ciências e Tecnologia, Universidade Nova de Lisboa, Caparica, Portugal. [5]BioMed X Institute (GmbH), Im Neuenheimer Feld 583, Heidelberg, Germany. [6]Oncology Division, Centro Hospitalar Barreiro-Montijo, Barreiro, Portugal. [7]Institute for Research on Cancer and Aging of Nice (IRCAN), UMR7284 U1081 UNS, Université Côte d'Azur, Nice, France. [8]Hemato-Oncologia Division, Hospital Garcia de Orta, Almada, Portugal. [9]Pathology Division, Hospital Garcia de Orta, Almada, Portugal. [10]Oncology Division, Hospital de Santa Maria, Centro Hospitalar Lisboa Norte, Lisbon, Portugal.

Note: Supplementary data for this article are available at Clinical Cancer Research Online (http://clincancerres.aacrjournals.org/).

Corresponding Authors: Marta Martins, Translational Oncology, Instituto de Medicina Molecular - João Lobo Antunes, Lisbon 1649-028, Portugal. E-mail: marta.martins@medicina.ulisboa.pt; and Luis Costa, Instituto de Medicina Molecular-João Lobo Antunes, Faculdade de Medicina, Universidade de Lisboa, Lisbon 1649-028, Portugal. E-mail: luiscosta.oncology@gmail.com

Clin Cancer Res 2022;XX:XX–XX

doi: 10.1158/1078-0432.CCR-21-1992

Translational Relevance

Cetuximab is a highly successful anti-EGFR mAb used in the treatment of patients with metastatic colorectal cancer (mCRC). However, its low rate of effectiveness suggests mechanisms of resistance so far undefined. Our discoveries identify a new mechanism of cetuximab resistance involving the EGFR effector PLCγ1 and its interaction with SHP2. Therefore, PLCγ1 IHC scoring in primary colorectal cancer samples identify patients resistant to cetuximab, but who simultaneously benefit from combined inhibition of SHP2 and EGFR. Overall, despite of an improved knowledge about the mechanisms of anti-EGFR therapeutic resistance, this work suggest novel clinical strategies for the treatment of patients with mCRC.

NRAS/BRAF/PIK3CA WT patients (10, 11). Nevertheless, cetuximab resistance among the quadruple WT population is still extremely high (around 58%; refs. 10, 11), suggesting the relevance of studying other EGFR intracellular signaling pathways as new biomarkers that can assist clinicians in the treatment decision-making in mCRC setting.

Similar to RAS, BRAF, and PI3K, PLCγ1 has long been characterized as a key element in intracellular signaling transduction downstream of receptor tyrosine kinases (RTK; refs. 12–14), such as EGFR, but its role in resistance to anti-EGFR therapies remains unexplored. PLCγ1 is a ubiquitously expressed enzyme that catalyzes the hydrolysis of the plasma membrane phospholipid phosphatidylinositol 4,5-bisphosphate (PIP2) into diacylglycerol (DAG) and inositol 1,4,5-trisphosphate (IP3; ref. 15). These two second-messengers are crucial regulators of many cellular processes, through the activation of DAG effectors, such as protein kinase C (PKC), and IP3-mediated Ca^{2+} release from intracellular stores.

Of note, PLCγ1 was shown to exert mitogenic functions downstream of EGFR (12, 16), and EGFR–PLCγ1 signaling was shown to be required for cell motility and invasion (17, 18). Furthermore, PLCγ1 has been associated with cancer development (16, 19, 20), and tumor progression and metastasis formation, including colorectal cancer (18–21). Importantly, activating mutations on the *PLCG1* gene were associated with resistance to sunitinib (multitarget RTK inhibitor) in hepatic angiosarcoma (22). Moreover, constitutive activation of PLCγ2 (the isoform predominantly expressed in hematopoietic cells) was also associated with resistance to the Bruton's tyrosine kinase (BTK) inhibitor (ibrutinib) in chronic lymphocytic leukemia (23).

This study was designed to elucidate the role of PLCγ1 in resistance to anti-EGFR therapies in mCRC, exploring its potential as a predictive biomarker of cetuximab response and its signaling pathway as a target of therapy.

Materials and Methods

RNA sequencing data analysis

Gene-based counts for TCGA COAD were downloaded from the GDC portal. Counts were normalized to obtain counts per million (CPM) values using the TMM normalization procedure in the edgeR R package (24). Somatic variants from Mutect for TCGA COAD were downloaded from the GDC portal. Genotyping array copy number variant calls estimates from GISTIC were also downloaded from GDC. RNA-seq data for PLCG1 expression levels from Asan Medical Center cohort were extracted from https://www.ncbi.nlm.nih.gov/geo/query/acc.cgi?acc=GSE50760.

Collection of drug sensitivity, gene expression, and mutation data

Drug sensitivity measurements were downloaded from the Cancer Dependency Map Portal https://depmap.org/portal/ as the sanger-dose-response.csv file from the Sanger GDSC1 and GDSC2 release. These data represented dose–response curve AUC measures (indicating the relationship between drug concentration and cell viability) for 974 cell lines across 398 compounds. Gene expression data were downloaded from https://depmap.org/portal/ as the CCLE_expression_full.csv file from the DepMap Public 20Q4 release. The file contained RNA-seq TPM gene expression quantification using RSEM for all genes across 1,375 cell lines from the Broad Institute Cancer Cell Line Encyclopedia (CCLE). Annotation of mutations in CCLE cell lines was downloaded from https://depmap.org/portal/ as the CCLE_mutations.csv file from the DepMap Public 20Q4 release.

Patient samples

Expression of PLCγ1 was evaluated by IHC in a retrospective cohort of 4 μm of formalin-fixed paraffin-embedded (FFPE) samples from human primary colorectal carcinomas from the Pathology Departments of three different hospitals: Hospital de Santa Maria (HSM-CHLN), Hospital Garcia da Orta (HGO), and Hospital Nossa Senhora do Rosário (CHBM). This study was conducted in accordance with recognized ethical guidelines (Declaration of Helsinki) and was approved by the Ethics Committee of all three hospitals. Written informed consent was obtained from all patients. Inclusion criteria were: patients with colorectal cancer diagnosed with metastatic disease from 2008 to 2018 who had been treated with cetuximab, and had a comprehensive clinical report including date of cetuximab treatments, date of dead, date of progression, chemotherapy-based regimes, and cetuximab-associated toxicity (Supplementary Table S1). From the 101 patients, 7 were excluded from analysis because, whereas being in remission under cetuximab, had surgery which left them without evidence of metastatic disease. Patients and treatment characteristics are summarized in Supplementary Table S1. Samples were analyzed by two independent pathologists, blinded for mCRC patients' clinical outcomes. Staining intensities were evaluated using the *H*-score method as described previously (25). For all samples, mutation status of codons 12, 13, 59, 61, 117, and 146 of both *KRAS* and *NRAS* and codon 15 of *BRAF* were evaluated by Sanger sequencing.

Cell culture, transfection, and infection

SW48, CACO-2, COLO320DM, and COS-7 cells were purchased from ATCC. LIM1215 cell line was purchased from Sigma-Aldrich. SW48 and COS-7 cell lines were cultured in DMEM (Gibco) supplemented with 10% (v/v) FBS (Gibco) and 1% (v/v) penicillin/streptomycin (Gibco). LIM1215 and COLO320DM were grown in RPMI1640 (Gibco) supplemented with 10% (v/v) FBS and 1% (v/v) penicillin/streptomycin. CACO-2 cell line was cultured in DMEM supplemented with 20% FBS, 10 mmol/L HEPES (Gibco), and 10 mmol/L nonessential amino acids (Gibco). Cells were maintained at 37°C with 5% CO_2, at low passage and routinely tested for mycoplasma contamination by qPCR (GATC Biotech). Cells lines were validated by short tandem repeat (STR) profile (STAB vida).

For PLCG1 knockdown, CACO-2 cells were infected with PLCG1 shRNA lentiviral particles and scrambled control (#sc-29452 and #sc-108080; Santa Cruz Biotechnology). Selection of stable clones started 2 days after infection with 10 μg/mL Puromycin (Sigma-Aldrich).

For overexpression of PLCG1 WT and mutants (H335A, D1019K, ΔSH2, and ΔSH3), SW48 cells were transfected with 0.5 μg of plasmid

DNA using Lipofectamine reagent 3000 (Invitrogen) following manufacturer's instructions.

For stable PLCG1 overexpression (SW48-PLCG1), SW48 cells were infected with PLCG1 lentiviral activation particles (#sc-400472-LAC; Santa Cruz Biotechnology). Selection of stable clones started 2 days after infection with a mix of 2 μg/mL Puromycin (Sigma-Aldrich), 50 mg/mL Hygromicyn B (Santa Cruz Biotechnology), and 10 mg/mL Blasticidin (InvivoGen).

Cloning

pTriex4 human full-length PLCG1 and mutants H335A and D1019K were gently provided by Dr. Matilda Katan (UCL, UK; ref. 15). Mutants of PLCγ1 comprising deletion of amino acids 545–759 (ΔSH2) and 791–870 (ΔSH3) were constructed by *in vitro* mutagenesis using the nzyMutagenesis Kit (NZYtech) according to manufacturer's instructions. Primer sequences used are the following:

ΔSH2 - GTCAGCAGCAGCAGCACAGAGCTGACAGCTGAGCCTGACTACG
ΔSH3 - GTAGAGGCAAACCCTATGCCAAACAGCCCCCTAGGGGACTTGC

All constructs include an N-terminal Hisx6 tag followed by an S-tag.

Cell viability, cell proliferation, caspase activity, and PLC activity assay

For cell viability, cells were seeded at a density of 1–2 × 10^4 in 96-well plates and treated with 0, 0.01, 0.1, 1, or 10 μg/mL of cetuximab (Erbitux), SHP inhibitor SHP099 (20 μmol/L; #10-4604–0005; Focus Biomolecules), and/or RAS inhibitor lonafarnib (10 μmol/L; #SML1457; Merck) for 72 hours. Following treatment, cell viability was assessed by adding 1:10 AlamarBlue reagent (Invitrogen) and fluorescence was measured 2 hours after incubation (excitation 560 nm; emission 590 nm) in Infinite M200 microplate reader (Tecan). Cell proliferation was measured using BrdUrd Cell Proliferation Assay Kit (#6813; Cell Signaling Technology). Measurement of caspase 3/7 activity was performed using the Apo-ONE Homogeneous 9 Caspase-3/7 Assay Kit (#G7790; Promega). PLC activity assay was performed as described previously (15).

Human phospho-kinase array

Cells were treated with cetuximab (Erbitux, 10 μg/mL) for 72 hours or left untreated, and the relative phosphorylation levels of 43 different kinases were measured using the Proteome Profiler Human Phosphokinase Array Kit (#ARY003B, R&D) according to manufacturer's instructions. Array membranes were incubated with 400 μg of cell lysate overnight at 4°C. Analysis and signal quantification was performed on scanned autoradiographic films and using ImageJ software.

EGFR surface expression

For evaluation of EGFR cell surface expression, cells were treated with cetuximab (10 μg/mL) for different time points (0 and 30 seconds, 1, 2, 24, and 72 hours) and fixed with 1% PFA (Merck) for 15 minutes. Specific mAb anti-EGFR Alexa Fluor 488-conjugated (#FAB9577G; R&D) was incubated on dark for 1 hour. Cells were washed in PBS with 0.1% FBS (FACS buffer), acquired on a BD LSRFortessa (BD Biosciences) and analyzed using FlowJo software (TreeStar).

EGFR internalization and degradation

Cells were transfected with Lipofectamine 3000 and incubated with cetuximab (Erbitux, 10 μg/mL) for different time points (0, 15, and 30 minutes). Cells were fixed in 4% PFA in PBS for 10 minutes at room temperature, permeabilized in 0.1% Triton-X100 in PBS for 10 minutes, and blocked in 3% BSA in PBS for 30 minutes. Primary antibodies: anti-PLCγ1 (#5690; Cell Signaling Technology), anti-EGFR Alexa Fluor 488-conjugated (#FAB9577G; R&D), and anti-LAMP-1/CD107a Alexa Fluor 647-conjugated antibody (#IC4800R; R&D) were incubated for 2 hours in the dark at room temperature. Secondary antibody (Goat anti-Rabbit IgG Alexa Fluor 568; #A-11011; Invitrogen) was incubated for 1 hour at room temperature in the dark. Nuclei was stained with DAPI (Sigma-Aldrich). Mowiol DABCO medium (Sigma-Aldrich) was used and images were obtained in a Zeiss LSM 710 confocal microscope.

Co-immunoprecipitation

For immunoprecipitation experiments, cells were lysed in 50 mmol/L Tris pH 7.5, 150 mmol/L NaCl (VWR), and 1% NP-40 (Sigma-Aldrich), sonicated with a single pulse of 15 seconds at 20% intensity using a Soniprep150 and digested with 5U DNase I (Promega) before preclearing with Protein G Dynabeads (Invitrogen) at 4°C for 30 minutes. Samples were diluted in immunoprecipitation buffer [20 mmol/L Hepes pH 7.0, 10 mmol/L KCl, 1.5 mmol/L $MgCl_2$, 0.2% (v/v) Tween20, 10% (v/v) glycerol, 1 mmol/L DTT] and incubated with antibodies (anti-S-Tag #12774; Cell Signaling Technology) and rabbit monoclonal anti-SHP2 (#3397, Cell Signaling) overnight at 4°C. The protein complexes were pulled-down using Protein G Dynabeads for 2 hours at 4°C and washed (20 mmol/L Hepes pH 7.0, 50 mmol/L KCl, 1.5 mmol/L MgCl2, 0.2% (v/v) Tween20, 10% (v/v) glycerol, 1 mmol/L DTT). Protein samples were eluted in 4× Laemmli buffer and resolved by Western blot analysis. One of 10 of the total cell lysate was used as input samples.

Proximity ligation assay (PLA)

SW48 cells were transfected and incubated with cetuximab (10 μg/mL) for 72 hours. PLA (Duolink in situ Fluorescence, Sigma-Aldrich) was used according to manufacturer's instructions. Specific primary antibodies rabbit monoclonal anti S-Tag (#12774; Cell Signaling Technology) and goat polyclonal anti-SHP2 (#ab9214) were used. To visualize the bound antibodies, the Duolink *in situ* PLA probes MINUS (#DUO92006) and PLUS (#92002) for rabbit and goat and Duolink *in situ* detection reagents Orange (#DUO92007) were used. Slides were mounted with Vectashield with DAPI (#H-1200) mounting medium. PLA dots were quantified using ImageJ particle analysis tool of four random fields per sample.

Zebrafish xenografts experiments

Zebrafish (*Danio rerio*) model was handled and maintained according to the standard protocols of the European Animal Welfare Legislation and Champalimaud Fish Platform. The experiments of this project were performed at the Champalimaud Vivarium, which is licensed by the National Authority for Animal Health (DGAV) and complies with European Guidelines (2010/63/EU), National Laws (113/2013), and FELASA guidelines. The study and procedures were approved by the Champalimaud Animal Welfare & Ethical Review Body (ORBEA) and DGAV. Zebrafish xenotransplant experiments were performed as described previously (26). Successful implanted xenografts were treated with cetuximab in E3 medium (100 μg/mL) or E3 medium plus DMSO (controls); the media were replaced daily. At 2 days postinjection (dpi), xenografts were exposed to SHP099 (20 μmol/L) when appropriate until the end of the assay. At 96 hours postinjection, zebrafish xenografts were fixed in 4% PFA at 4°C overnight. Whole-mount immunofluorescence technique was performed with anti-Ki-67 (#NCL-L-Ki67-MM1; Leica Biosystems),

rabbit monoclonal anti-cleaved Caspase-3 (Asp175; #CST9661, Cell Signaling Technology), and secondary antibodies (Alexa goat anti-mouse 488 and Alexa goat anti-rabbit 647; Thermo Fisher Scientific) plus DAPI to counterstain nuclei. Xenografts were mounted with mowiol mounting media and imaged in a Zeiss LSM 710 confocal microscope. All data presented were normalized to the control.

Statistical analysis

GraphPad Prism version 8 and SPSS software was used to perform statistical analysis. Spearman correlation, paired, unpaired *t* test, or one-way ANOVA were used for *in vitro* data, as indicated in the text and figure legends. Median OS and PFS were obtained using Kaplan–Meier methods, and log-rank test was used to compare group outcomes. Cox regression model was used to perform univariate and multivariate assessment of the effect of investigated parameters in the duration of response and prognosis. All statistical tests were two-tailed. The association between PLCγ1 expression and patients' clinicopathological features was accessed by Chi-square or Fisher exact tests, depending on the variable number, as referred in the legend of Supplementary Table S1. For zebrafish experiments, all data were challenged by Shapiro–Wilk and D'Agostino & Pearson normality tests. A Gaussian distribution was only assumed for datasets that pass both normality tests and were analyzed by an unpaired *t* test with Welch correction. Datasets without Gaussian distribution were analyzed by unpaired and nonparametric Mann–Whitney test. For metastasis incidence analysis, the Fisher exact test was used. Results are presented as mean ± SEM. The level of statistical significance was set as nonsignificant (NS); *, $P < 0.05$; **, $P < 0.01$; ***, $P < 0.001$; and ****, $P < 0.0001$. For all the statistical analyses, *P* value (*P*) is from a two-tailed test with a confidence interval of 95%.

Data availability

This study includes no data deposited in external repositories.

Results

PLCγ1 is upregulated in *RAS* WT colorectal cancer tumors and metastases

PLCγ1 is a signaling effector of EGFR whose expression was shown to be altered in solid tumors, including colorectal cancer (21). To investigate the relevance of PLCγ1 in the context of resistance to EGFR-targeted therapies, we started by analyzing the landscape of *PLCG1* alterations in a dataset of 445 colorectal cancer samples from The Cancer Genome Atlas (TCGA-COAD; ref. 27). In this cohort, approximately 70% of tumors harbor alteration on *APC* gene, 50% on *RAS* (*KRAS* and *NRAS*), 30% on *PIK3CA*, 17% on *BRAF*, 10% on *CCTNB1*, 6% on *EGFR*, and 9% on *PLCG1* gene (Supplementary Fig. S1A). Regarding *PLCG1* gene modifications, less than 1% corresponds to deletions, 3% to nonsynonymous mutations, and 5% refers to gene amplification (Supplementary Fig. S1A). Accordingly, *PLCG1* expression levels were found increased in tumors with gene amplification when compared with *PLCG1* WT and deleted tumors ($^{**}P < 0.01$ and $^{*}P < 0.05$, respectively; Supplementary Fig. S1B). Furthermore, 80% of colorectal cancer samples with amplification on *PLCG1* gene display *APC* gene alterations, as well as 9% show mutation on *CCTN* gene and 5% exhibit alterations on *EGFR* gene, which reflects the frequency of the entire cohort (Supplementary Fig. S1A). Importantly, cetuximab is only eligible to *RAS* WT tumors, which are highly frequent (∼95%) in *PLCG1* amplified samples, suggesting that a great number of cetuximab-treated patients express high levels of PLCγ1. Therefore, *PLCG1* mRNA levels were investigated in *RAS* WT tumors and normal colonic mucosa in TCGA-COAD dataset (27). Results show that PLCγ1 is upregulated in *RAS* WT tumors when compared with normal tissue (****, $P < 0.0001$; **Fig. 1A**). To validate this result, we analyzed an independent dataset of 13 pairs of normal, *RAS* WT colorectal cancer tumors and liver metastases, from the Asan Medical Center (AMC; ref. 28). *PLCG1* expression was confirmed higher in *RAS* WT tumors than matched normal samples (*, $P < 0.05$; **Fig. 1B**). However, comparison between primary tumors and matched metastases showed no significant difference on *PLCG1* expression, suggesting that metastases mimic primary tumors regarding PLCγ1 expression (**Fig. 1B**).

Overall, these results indicate that alterations in *PLCG1* gene such as deletions and nonsynonymous mutations are uncommon in colorectal cancer. Furthermore, *PLCG1* gene amplifications, although occurring only in about 5% of colorectal cancer samples, seem predominant in *RAS* WT tumors (Supplementary Fig. S1A). In addition, *PLCG1* mRNA expression levels are frequently upregulated in *RAS* WT colorectal cancer tumors and metastases (**Fig. 1A** and **B**), suggesting an important role of PLCγ1 levels in colorectal cancer development and progression, with potential relevance in therapy resistance.

Levels of PLCγ1 associate with resistance to cetuximab *in vitro*

Considering the previous results, we evaluated the impact of PLCγ1 expression levels in cetuximab responses *in vitro*. Using the Genomics of Drug Sensitivity in Cancer (GDSC; refs. 29–31) and the Cancer Cell Line Encyclopedia (CCLE) databases (32, 33), we analyzed a panel of 14 colorectal cancer *RAS* WT cell lines and their respective values of *PLCG1* expression and cetuximab sensitivity (measured as the area under the curve or AUC). A positive correlation was found between *PLCG1* expression and cetuximab resistance (Spearman correlation coefficient = 0.5516; *, $P = 0.0418$; **Fig. 1C**). These cell lines were further dichotomized in *PLCG1*-low and *PLCG1*-high by the average value of *PLCG1* expression. Comparison between both groups showed that colorectal cancer *RAS* WT cell lines expressing higher levels of PLCγ1 have increased resistance to cetuximab (*, $P = 0.013$; **Fig. 1D**).

Moreover, PLCγ1 levels were analyzed by Western blotting in an independent panel of cetuximab-sensitive (LIM1215 and SW48) and cetuximab-resistant (CACO-2 and COLO320DM) *RAS* WT colorectal cancer cell lines (34, 35). Exposure of cells to cetuximab confirmed reported sensitivity and showed that PLCγ1 expression was higher in resistant compared with sensitive cell lines (**Fig. 1E** and **F**). Interestingly, neither Y783 phosphorylation (critical for its lipase activation), nor activation of the PLCγ1 downstream effector PKC, correlate with resistance to cetuximab (**Fig. 1F**). These suggest that, although PLCγ1 levels may be important for cetuximab sensitivity, its role seems independent of its catalytic activity.

To functionally validate the role of PLCγ1 in cetuximab response, *PLCG1* was knocked-down by shRNA in the most resistant cell line CACO-2 and ectopically overexpressed in the most sensitive cell line SW48. Although PLCγ1 overexpression reduced sensitivity (*, $P = 0.0372$), PLCγ1 deletion sensitized cells to cetuximab (**Fig. 1G–L**; *, $P = 0.0201$). These results confirm that PLCγ1 levels contribute to cetuximab responses. Furthermore, PLCγ1 expression was found to mediate cell viability in response to cetuximab through positive proliferation (BrDU) and negative apoptotic regulation (caspase 3/7 activity; **Fig. 1G–L**).

Taken together, these results indicate that high levels of PLCγ1 contribute to cetuximab resistance in *RAS* WT colorectal cancer cell lines, whereas PLCγ1 ablation reverts the resistant phenotype and sensitizes cancer cells to cetuximab treatments.

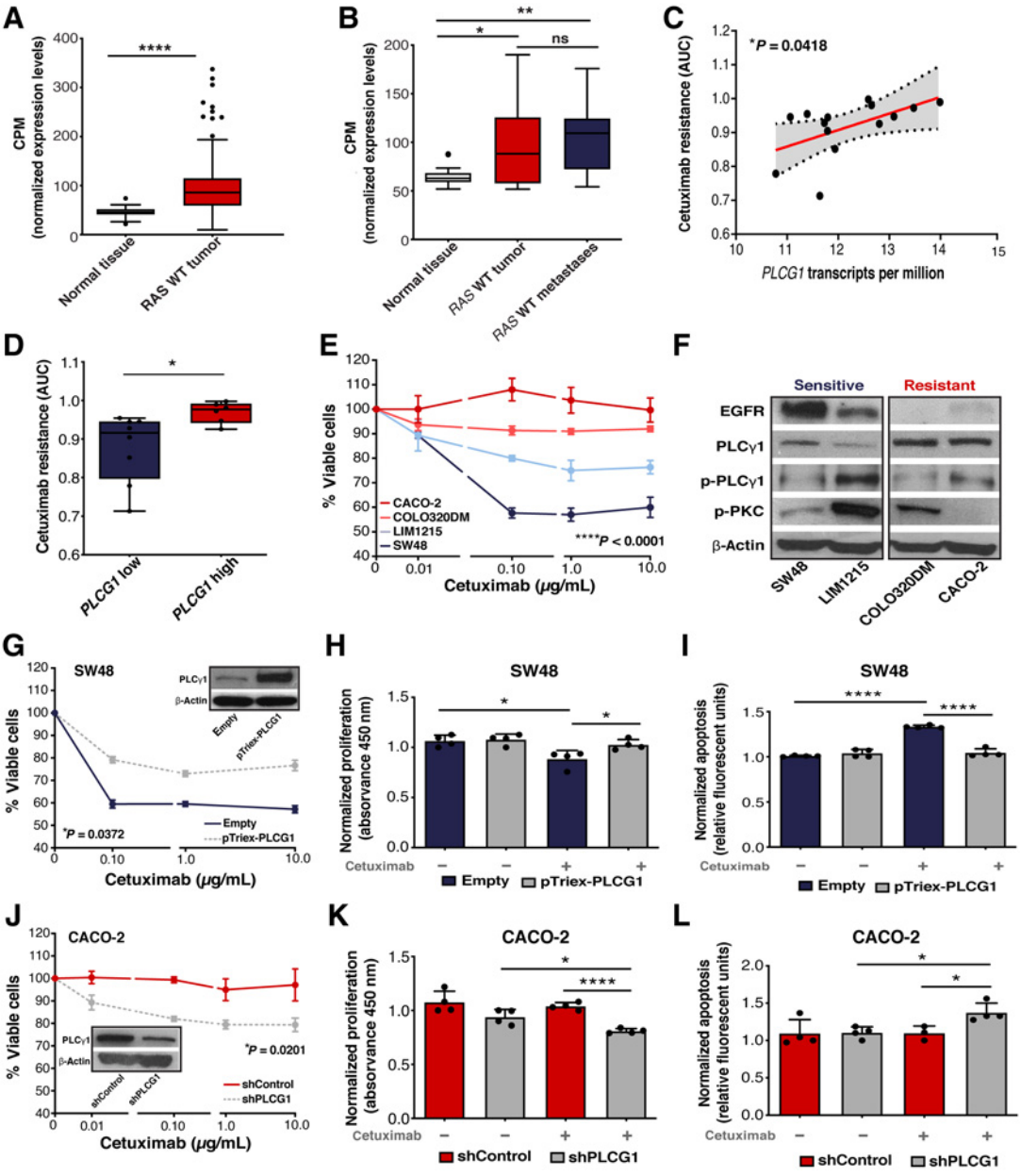

Figure 1.

PLCγ1 expression in colorectal cancer and its association with cetuximab responses. **A,** Comparison of *PLCG1* mRNA expression levels in *RAS* WT tumors ($n = 273$) versus normal colonic mucosa ($n = 41$) from TCGA-COAD dataset. **B,** *PLCG1* mRNA expression of paired *RAS* WT tumors, normal samples, and liver metastasis from AMC cohort ($n = 13$). **C,** Correlation between the levels of *PLCG1* expression [RNA-seq TPM gene expression quantification from the Broad Institute Cancer Cell Line Encyclopedia (CCLE)] and cetuximab resistance (drug sensitivity measurements of GDSC from the Cancer Dependency Map Portal) in colorectal cancer *RAS* WT cell lines ($n = 14$). *P* value corresponds to the Spearman correlation test. Drug sensitivity was measured as AUC which corresponds to the AUC in which values of 0 correspond to complete reduction in cell viability and values of 1 correspond to no reduction in cell viability. Fitted linear regression line and its 95% CIs are indicated by the red line and shaded area, respectively. **D,** Cetuximab resistance of *RAS* WT colorectal cancer cell lines grouped by low or high *PLCG1* expression based on the analysis of GDSC and CCLE data ($n = 14$; unpaired *t* test). **E,** Cell viability of colorectal cancer cell lines measured 72 hours after initial exposure to cetuximab ($n = 4$, two-way ANOVA test). **F,** Western blotting of EGFR and PLCγ1 downstream signaling. β-Actin was used as the loading control. **G–I,** Cell viability ($n = 4$, two-way ANOVA test), proliferation, and apoptosis rate of parental and *PLCG1* overexpressing SW48 cells (pTriex-PLCG1) upon 72 hours of treatment with cetuximab (unpaired *t* test). **J–L,** Cell viability ($n = 4$, two-way ANOVA test), proliferation, and apoptosis rate of shControl and shPLCG1 CACO-2 cell line after 72 hours of treatment with cetuximab (unpaired *t* test). Results are presented as the mean ± SEM. (*, $P \leq 0.05$; **, $P \leq 0.01$; ****, $P \leq 0.0001$).

PLCγ1 expression favors tumor progression under cetuximab treatment

Zebrafish has been used as a xenotransplant cancer model, not only to estimate cancer behavior, but also to test therapy efficacy (26, 36). Importantly, we previously showed that this model revealed a remarkable sensitivity to detect differential responses to cetuximab using both cell lines and patient-derived xenografts (zPDX; ref. 26). Therefore, to investigate further the above results, CACO-2 and SW48 cells stably expressing low and high levels of PLCγ1, respectively, were labeled with a lipophilic dye (DiI) and xenotransplanted into the perivitelline space (PVS) of 48-hour postfertilization (hpf) zebrafish embryos (**Fig. 2A**; Supplementary Fig. S2A and S2B). At 4 dpi, zebrafish xenografts were fixed and prepared for confocal immunofluorescence analysis to quantify the impact of cetuximab treatment in tumor cell dynamics (tumor size, cell death, cell proliferation, and metastasis formation). In agreement with the results described above, we found that cetuximab treatment of CACO-2 shControl tumors do not impact on their tumor size nor activated caspase 3, confirming its resistance to cetuximab (P = ns; **Fig. 2B**, **B'**, **D**, **D'**, **F**, and **G**). In contrast, CACO-2 shPLCG1 tumors show a significant reduction of tumor size and induction of activated caspase 3 when treated with cetuximab (∼21% reduction of tumor size; *, $P = 0.0387$, and ∼2-fold increase of apoptosis; ****$P < 0.0001$; **Fig. 2C–C'**, **E–E'**, **F**, and **G**). Of note, knocking-down PLCγ1 expression significantly impaired proliferation of both untreated (***$P < 0.001$) and cetuximab-treated tumors (**** $P < 0.0001$) measured by Ki-67 staining (**Fig. 2B"**, **C"**, **D"**, **E"**, and **H**), which is in agreement with a relevant role of PLCγ1 in colorectal cancer development. Nevertheless, direct comparison of cetuximab effect on shControl versus shPLCG1 tumors showed marked induction of apoptosis (∼2-fold increase in apoptosis; ****$P < 0.0001$;

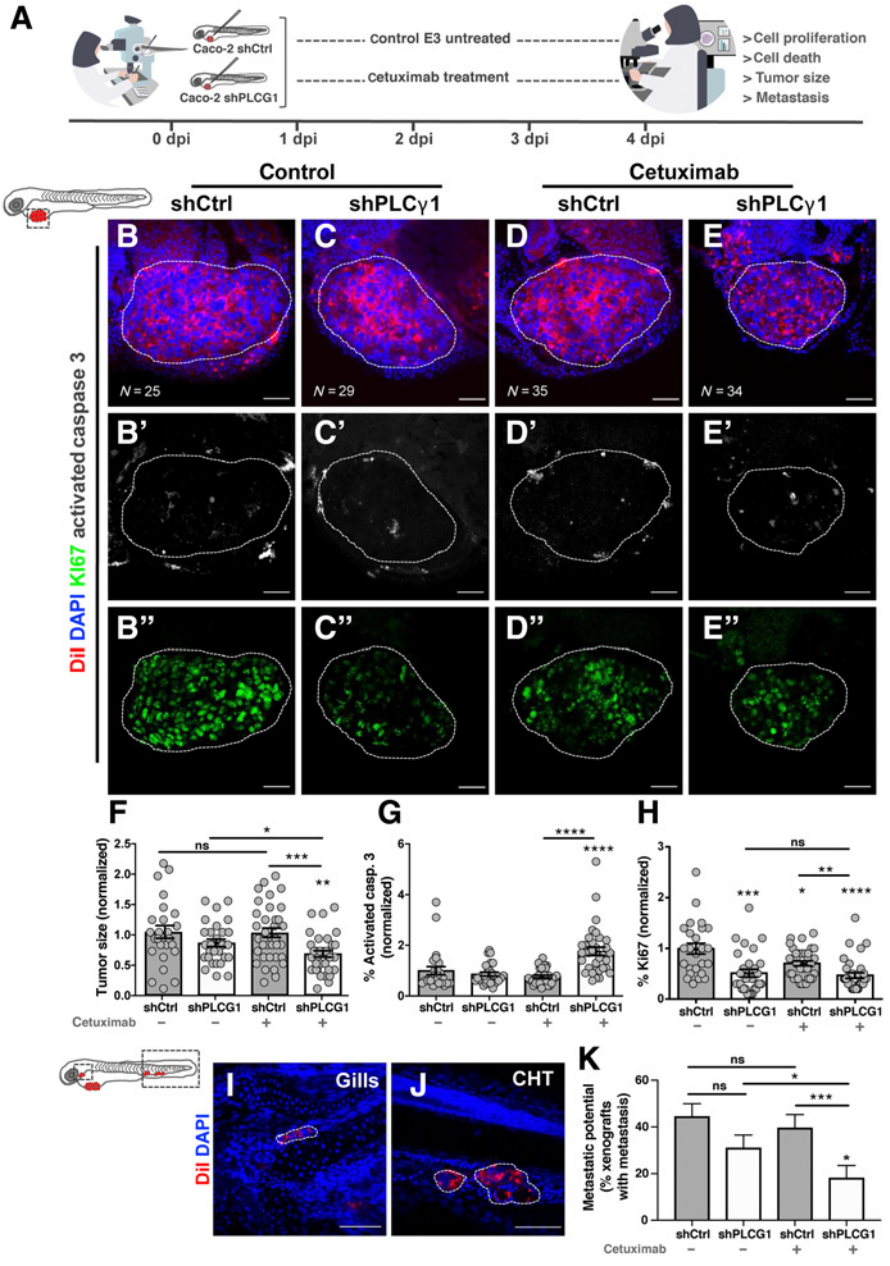

Figure 2.

Zebrafish xenotransplant model of shControl and shPLCG1 CACO-2 cells treated with cetuximab. **A,** Human cancer cell line CACO-2 (shCtrl and shPLCG1) was fluorescently labeled with DiI (red) and injected into the perivitelline space (PVS) of 2 days postfertilization (dpf) *nacre/casper* zebrafish larvae. Zebrafish xenografts were treated *in vivo* with cetuximab for 72 hours and compared with untreated controls regarding tumor size, cell death, cell proliferation, and metastasis formation. **B–E",** At 4 dpi, zebrafish xenografts were imaged on PVS and over the zebrafish body by confocal microscopy. **F,** Analysis of tumor size (*, $P = 0.0387$; **, $P = 0.0063$; ***, $P = 0.0007$). **G,** Analysis of activated caspase 3 (apoptosis; ****, $P < 0.0001$). **H,** Percentage of Ki-positive cells (*, $P = 0.0191$; **, $P = 0.0021$; ***, $P = 0.0001$; ****, $P < 0.0001$). **I** and **J,** Representative images of CACO-2 micrometastasis. **K,** Metastasis quantification (shPLCG1 versus shPLCG1 cetuximab *$P = 0.0238$, shCTRL versus shPLCG1 cetuximab *$P = 0.0124$, shCTRL cetuximab versus shPLCG1 cetuximab ***$P = 0.0004$). The outcomes are expressed as AVG ± SEM. Results are from two independent experiments and the number of xenografts analyzed are indicated in the representative images. Each dot represents one zebrafish xenograft. Statistical analysis was performed as described in Statistical Analysis section (ns > 0.05; *, $P \le 0.05$; **$P \le 0.01$; ***$P \le 0.001$, ****$P \le 0.0001$). Scale bars represent 50 μm. All images are anterior to the left, posterior to right, dorsal up, and ventral down.

Fig. 2D', **E'**, and **G**) associated with a reduction of about 34% of tumor size of shPLCG1 tumors (***$P = 0.0007$; **Fig. 2D–D"**, **E–E"**, and **F**).

On the other hand, SW48-sensitive tumors showed a reduction of about 40% of tumor mass (****$P < 0.0001$), ∼3-fold increase in apoptosis (measured by activated caspase 3, ****$P < 0.0001$) and 15% decrease in proliferation (*$P = 0.0134$) when treated with cetuximab (Supplementary Figs. S2C–S2C", S2E–S2E", S2G, S2H, and S2I). Stable overexpression of PLCγ1 in these cells (SW48-PLCγ1; Supplementary Fig. S2B) rendered cetuximab treatment ineffective in inducing alteration of tumor size, apoptosis, or proliferation (Supplementary Figs. S2D–S2D", S2F–S2F", S2G, S2H, and S2I). In general, upon cetuximab treatment, SW48-PLCγ1 tumors are about 40% bigger than SW48 tumors, showing approximately 3 times lower apoptosis and ∼30% higher proliferation (****$P < 0.0001$, Supplementary Figs. S2E–S2E", S2F–S2F", S2G, S2H, and S2I). Overall, these results confirm that PLCγ1 expression leads to resistance of tumor cells to anti-EGFR therapy.

Importantly, cetuximab treatment is mainly administrated during metastatic disease to control progression, therefore the impact of cetuximab in metastases development is also an important feature to be addressed. The zebrafish xenograft assay provides this opportunity given that at 4 dpi human fluorescently labeled tumor cells can be found in distant sites such as brain, optic cup, gills, and caudal hematopoietic tissue (CHT; refs. 26, 36). Quantification of the number of xenografts with micrometastasis revealed that under cetuximab treatment, CACO-2 shPLCG1 tumors had a reduced capacity to colonize secondary tissues when compared with CACO-2 shControl cells (∼60% reduction of micrometastasis, ***$P < 0.001$; **Fig. 2I–K**). Instead, cetuximab-sensitive SW48 cells showed increased ability to form metastasis when PLCγ1 was overexpressed (∼75% increase in micrometastasis formation upon cetuximab treatment; ****$P < 0.0001$; Supplementary Fig. S2J–S2L).

Altogether, these results indicate that PLCγ1 levels affect not only tumor growth, but also the ability of cancer cells to colonize distant sites upon cetuximab treatment. Remarkably, loss of PLCγ1 expression can significantly increase cetuximab sensitivity.

PLCγ1 expression levels predict cetuximab resistance in colorectal cancer human samples

Considering these results, we examined the value of PLCγ1 expression in predicting cetuximab responses in the clinical setting. For that, PLCγ1 levels were assessed by IHC in a retrospective cohort of 94 *RAS* WT colorectal cancer samples from patients with mCRC treated with cetuximab from three different hospitals in Portugal: Hospital de Santa Maria (HSM-CHLN), Hospital Garcia da Orta (HGO), and Hospital Nossa Senhora do Rosário (CHBM). For analysis, progression-free survival (PFS) was considered as the length of time from the beginning of cetuximab treatment until: (i) progression (defined by radiographic assessment or clinically), (ii) end of cetuximab due to severe toxicity, or (iii) death.

Overall survival (OS) was measured as the length of time from the start of cetuximab therapy until patients' death. This cohort displayed a median PFS of 6.4 months, OS of 15.5 months, and median follow up of 20.1 months.

Cytoplasmic immunoreactivity was evaluated in paraffin-embedded primary tumors using the *H*-score method (**Fig. 3A**; ref. 25). PFS analysis by quartiles of PLCγ1 expression [Q1 (0%–25%), Q2 (25%–50%), Q3 (50%–75%), and Q4 (75%–100%)] showed a significant trend that higher-expression patients progress faster under cetuximab therapy (log-rank test for trend, *$P = 0.0340$), with a clear distinction between Q1–2 versus Q3–4 patients (Supplementary Fig. S1C and S1D). These result suggest that the median value of the *H*-score can separate patients into two groups with distinct outcomes. Therefore, patients were dichotomized by the median value of the final *H*-score into PLCγ1-low and PLCγ1-high expression. A total of 43.6% of patients had low and 56.4% high PLCγ1 expression, being both groups balanced for the clinicopathologic features depicted in Supplementary Table S1. Therefore, PFS analysis showed that patients with cetuximab-treated mCRC with higher levels of PLCγ1 expression progress 1.6 months faster than patients with lower PLCγ1 expression (log-rank *$P = 0.0181$; HR, 0.6186; 95% CI, 0.393–0.901; **Fig. 3B**). Median PFS was 7.1 months for low and 5.5 months for high PLCγ1 expression patients (**Fig. 3C**), suggesting that PLCγ1 levels inversely correlate with cetuximab response. Cox regression model of univariate and multivariate analyses confirm the predictive value of PLCγ1 expression (*$P = 0.019$; HR, 1.68; 95% CI, 1.09–2.60; **$P = 0.005$; HR, 1.95; 95% CI, 1.22–3.11, respectively) without association of other biological markers, such as BRAF mutations, with cetuximab progression (Supplementary Table S2). OS analysis showed no significant difference between low or high PLCγ1 expression patients (log-rank $P = 0.1471$; HR, 0.7392; 95% CI, 0.473–1.02; **Fig. 3D** and **E**), which can be justified by the subsequent lines of therapy that patients follow after progressing from cetuximab, which highly impact on their OS. Taken together, these results from independent cohorts strongly suggest that PLCγ1 expression predicts cetuximab resistance in *RAS* WT patients with mCRC.

PLCγ1 regulates responses to cetuximab through ERK and AKT signaling

Cetuximab is an anti-EGFR mAb that inhibits EGFR function (5). PLCγ1 binds to EGFR and transduces some of its intracellular signals. Therefore, to investigate the mechanism behind PLCγ1 contributions to cetuximab responses, we analyzed the role of PLCγ1 expression on EGFR behavior and on EGFR downstream signaling, upon cetuximab treatment. For that, flow cytometry and immunofluorescence analysis of EGFR expression were performed in SW48 and CACO-2 cells. In 72 hours of cetuximab exposure, EGFR levels both at the membrane and internal endosome vesicles (LAMP1 stained) showed no significant differences between PLCγ1-high and PLCγ-low expressing cells (Supplementary Fig. S3A–S3C). Furthermore, Western blotting of total EGFR levels in these cell lines do not correlate with PLCγ1 expression (**Fig. 4A** and **B**), suggesting that PLCγ1 mediates cetuximab response without modifying EGFR expression, internalization, or degradation rates.

Interestingly, EGFR levels analyzed by flow cytometry and Western blotting remained unmodified in CACO-2 cells upon cetuximab treatment (Supplementary Fig. S3B; **Fig. 4A**). In contrast, in SW48 cells, EGFR becomes significantly downregulated by the treatment (Supplementary Fig. S3A; **Fig. 4B**). Remarkably, independently of EGFR levels, downstream ERK and AKT activation correlates with PLCγ1 expression in cetuximab-treated cells (**Fig. 4A** and **B**).

Therefore, these results suggest that, upon cetuximab treatment, PLCγ1 mediates ERK and AKT activation, rather than regulation of the receptor itself. In support of this mechanism, previous reports have shown that PLCγ1 could signal through ERK and AKT (37, 38), which are both positive regulators of cell proliferation and survival associated with resistance to cetuximab (10, 11, 39).

SH2 tandem domains are essential for PLCγ1-mediated downstream signaling under cetuximab therapy

PLCγ1 is a multidomain protein that contains a catalytic region consisting of an N-terminal PH domain, EF-hands, X and Y TIM-like

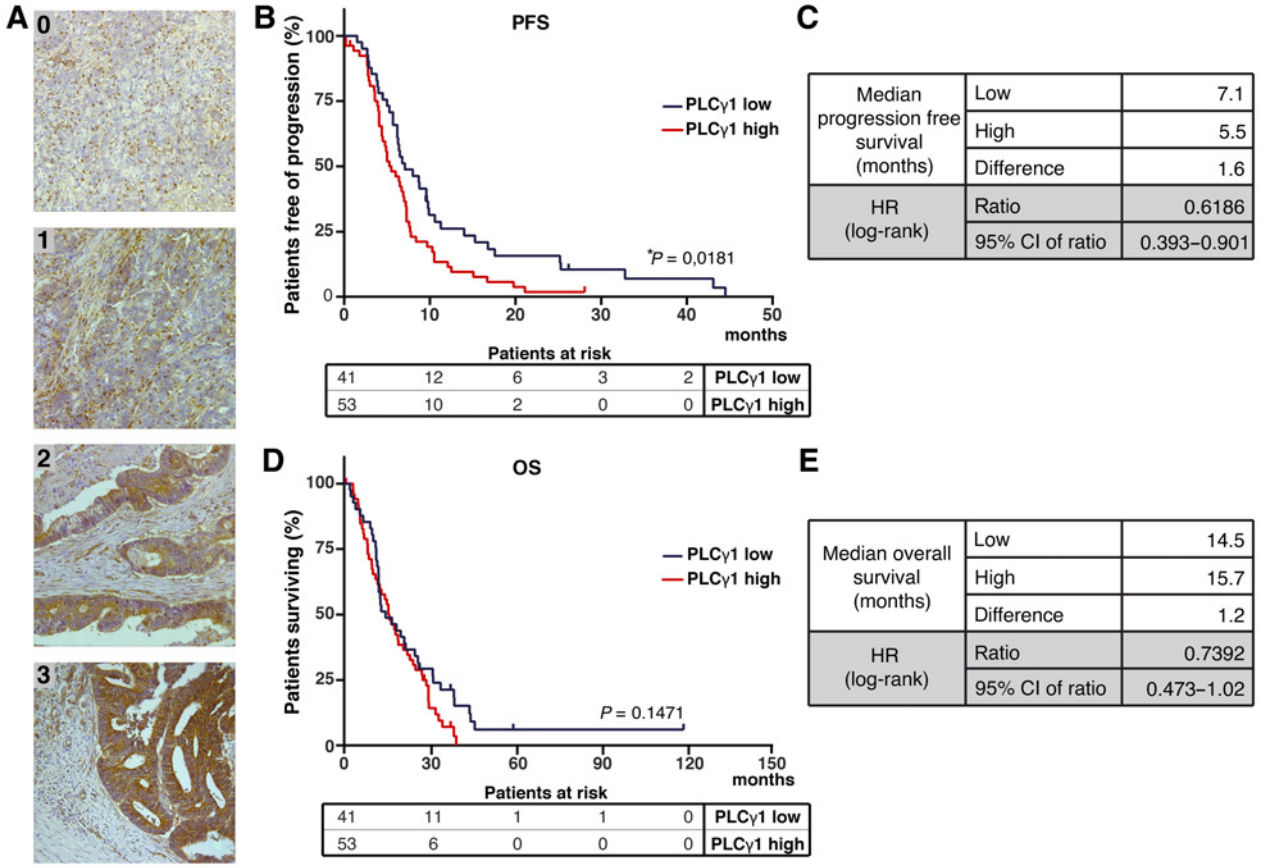

Figure 3.

PLCγ1 expression in colorectal cancer tumors and its association with cetuximab responses. **A,** IHC analysis of PLCγ1 expression in human colorectal cancer specimens. Intensity of PLCγ1 cytoplasmic staining in tumor cells ranges from 0 (absence of staining) to 3 (maximal intensity; magnification, 200×). **B–E,** Kaplan–Meier curves of PFS and OS of patients with colorectal cancer expressing high and low levels of PLCγ1. Median time of survival for both analyses is shown in the picture. *P* value of the Kaplan–Meier curves was calculated using the log-rank test.

barrel and a C2 domain (Supplementary Fig. S4A; ref. 15). Inserted within the X and Y TIM-like barrel domains is the regulatory region that consists of a split PH domain (important for maintaining auto-inhibition), two SH2 domains (nSH2-cSH2, important for recognition of phospho-tyrosine motifs), and an SH3 domain (important for recognition of polypeptide motifs; ref. 15). To determine which domain is essential for PLCγ1-mediated responses to cetuximab, several PLCγ1 mutants were expressed on sensitive SW48 cells: D1019K- PLCγ1 constitutively active; H335A- PLCγ1 inactive; ΔSH2- deletion of nSH2-cSH2 domains; and ΔSH3- deletion of SH3 domain (Supplementary Fig. S4B; **Fig. 4C**). Western blotting analysis demonstrates that all mutants are expressed, and inositol phosphate formation in COS-7 cells confirmed that D1019K mutant is active, whereas H335A is a lipase death mutant (Supplementary Fig. S4B and S4C). Moreover, deletion of SH2 tandem auto-inhibitory domain was seen to induce PLCγ1 lipase activation (Supplementary Fig. S4C), as reported previously (15).

Expression of mutants in SW48 cells showed that H335A inactive mutant was still able to induce resistance to cetuximab, similarly as the PLCγ1 full length WT (**Fig. 4C**). This indicates that PLCγ1 catalytic activity is dispensable for cetuximab-induced resistance, as in agreement with our initial observations that pPLCγ1 and pPKC were irrelevant for cetuximab resistance (**Fig. 1F**). Surprisingly, although showing increased lipase activity (Supplementary Fig. S4C), PLCγ1 ΔSH2 mutant was unable to elicit cetuximab resistance in SW48 cells (**Fig. 4C**). Moreover, Western blotting analysis confirmed that nSH2-cSH2 domains are crucial for PLCγ1-dependent ERK and AKT activation and hence for cetuximab responses (**Fig. 4D**).

Furthermore, PLCγ1 SH2 domains were found essential for MEK activation in cetuximab-treated cells, which is the upstream regulator of ERK (**Fig. 4D**). To explore further PLCγ1-mediated signaling, RAS activation status was analyzed by GTP-RAS pull down. Contrarily to PLCγ1 WT, overexpression of ΔSH2 mutant in SW48 cells was unable to sustain RAS activation during cetuximab therapy (**Fig. 4D**). Moreover, inhibition of RAS farnesylation by lonafarnib (essential step for RAS functional activation) reverts PLCγ1 WT-resistant phenotype in these cells to levels of PLCγ1 ΔSH2 (Supplementary Fig. S5A), suggesting that PLCγ1-mediated responses to cetuximab involve RAS signaling transduction in a SH2-dependent way.

For a deeper understanding of the signaling profile of PLCγ1-dependent cetuximab-resistant cells, a phospho-kinase array was developed comparing SW48 cells expressing PLCγ1 WT and ΔSH2 mutant. Several pathways involved in proliferation, inflammation, differentiation, glucose regulation, and migration, such as ERK1/2, JNK1/2/3, GSK-3, AKT, mTOR, and STAT5, remain unchanged in PLCγ1-expressing SW48 cells upon cetuximab treatment

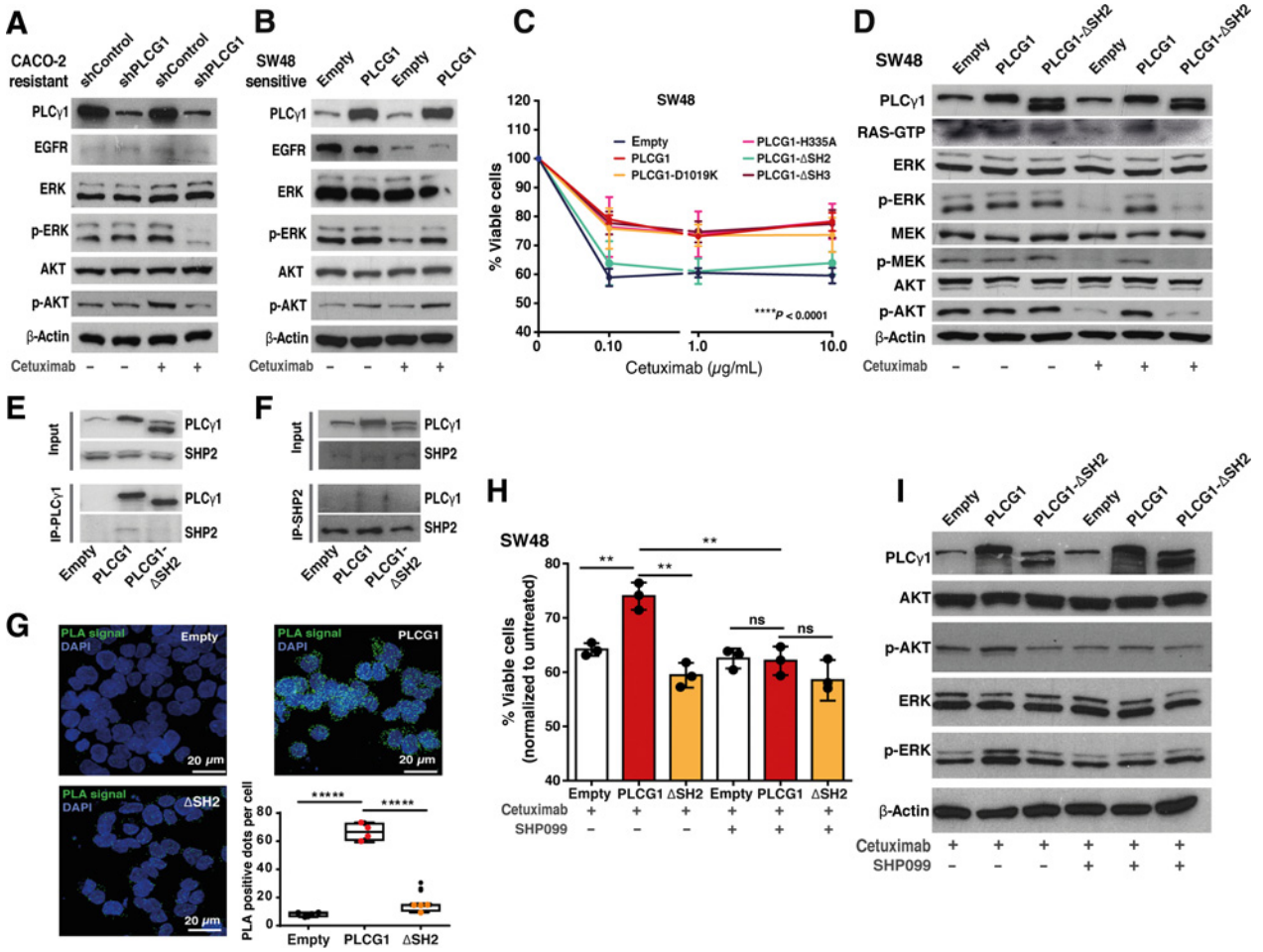

Figure 4.

Role of PLCγ1 nSH2-CSH2 domains and its interaction with SHP2 for cetuximab resistance. **A** and **B,** Western blotting of CACO-2 (shControl and shPLCG1) and SW48 (parental and pTriex-PLCG1 overexpressed) cells treated with cetuximab for 72 hr. EGFR downstream signaling, namely ERK and AKT are shown. β-actin was used as the loading control. **C,** Cell viability of parental SW48 and PLCG1-overexpressing cells: full length WT; constitutively active mutant - D1019K; constitutively inactive mutant - H335A; deletion of both nSH2-CSH2 tandem domains - ΔSH2; and deletions of SH3 domain - ΔSH3 ($n = 3$). Analysis was performed using two-way ANOVA test (****$P < 0.0001$). **D,** Western blotting of EGFR downstream signaling of SW48 parental and overexpressing *PLCG1* WT and *PLCG1* ΔSH2 mutant, after 72 hr of cetuximab treatment. β-Actin was used as the loading control. **E,** Co-immunoprecipitation of PLCγ1 with anti-Stag antibody and Western blot analysis of PLCγ1 and SHP2 of 72 hours cetuximab treated SW48 cells. **F,** Co-immunoprecipitation of SHP2 with anti-SHP2 antibody and Western blot analysis of PLCγ1 and SHP2 of 72 hours cetuximab treated SW48 cells. **G,** Proximity ligation assay of PLCγ1 and SHP2 using anti-Stag and anti-SHP2 antibodies in SW48 parental, PLCG1 WT- and ΔSH2-overexpressing cells and corresponding quantification ($n = 4$). **H,** Cell viability of SW48 parental and overexpressing PLCG1 WT and ΔSH2 mutant, treated with cetuximab and cetuximab + SHP099 for 72 hours ($n = 3$). **I,** Western blotting of EGFR downstream signaling of SW48 parental and overexpressing PLCG1 WT and ΔSH2 mutant, treated with cetuximab and cetuximab + SHP099. Results are presented as the mean ± SEM. Statistical analysis was performed using unpaired *t* test [not significant (ns), $P > 0.05$; **, $P < 0.01$].

(Supplementary Fig. S5B). In contrast, the same kinases become dephosphorylated by cetuximab treatment in ΔSH2-expressing SW48 sensitive cells (Supplementary Fig. S5C), indicating that expression of PLCγ1 is crucial to maintain cancer-associated signaling pathways under cetuximab therapy, in a SH2-dependent way.

Interestingly, phosphorylation of p53 residues S392 and S46, which are associated with pro-apoptotic function, were found reduced in PLCγ1-expressing cells upon cetuximab treatment (Supplementary Fig. S5B). On the contrary, ΔSH2 SW48 expressing cells show an increase in phosphorylation of these p53 residues upon cetuximab treatment (Supplementary Fig. S5C). Thus, despite PLCγ1 functions in holding survival, proliferative, and migratory signals, it also has an important role in apoptosis evasion upon cetuximab treatment, as in agreement with the zebrafish xenotransplant *in vivo* model described above (**Fig. 2**; Supplementary Fig. S2).

PLCγ1 nSH2-cSH2 domains are necessary for SHP2 binding under cetuximab therapy

SH2 domains are phospho-tyrosine (pY) binding motifs (40). Therefore, using co-immunoprecipitation (co-IP), we investigated whether PLCγ1 could bind to RAS upstream regulators such as SOS, Grb2, and SHP2 under cetuximab therapy. Remarkably, only SHP2 was found to co-immunoprecipitate with PLCγ1 in an nSH2-cSH2–dependent way, under cetuximab treatment (**Fig. 4E** and **F**). To validate PLCγ1–SHP2 binding in live cells, a proximity ligation assay

(PLA) was conducted, which confirmed that under cetuximab treatment PLCγ1 binds to SHP2 in colorectal cancer cells via its SH2 tandem domains (**Fig. 4G**). These results suggest that SHP2 can be a potential partner of PLCγ1-mediated RAS activation in colorectal cancer cells exposed to cetuximab.

SHP2 inhibition sensitizes PLCγ1-expressing cells to cetuximab treatment

SHP2 is a core component of a multiprotein complex that promotes RAS activation downstream of various RTKs (41). To test the role of SHP2 on PLCγ1-mediated RAS activation upon cetuximab treatment, SW48 cancer cells overexpressing PLCγ1 and ΔSH2 mutant were exposed to the potent and selective SHP2 allosteric inhibitor SHP099. Combined SHP099 and cetuximab treatment was found to abolish resistance to this anti-EGFR agent induced by PLCγ1 expression (**Fig. 4H**). Western blotting analysis revealed that cotreatment of SW48 cells prevent PLCγ1-mediated ERK and AKT activation (**Fig. 4I**), suggesting that SHP2 is a downstream partner of PLCγ1 in cetuximab resistance.

To test whether inhibition of SHP2 could sensitize CACO-2 and SW48-PLCγ1–resistant cells to cetuximab *in vivo*, the zebrafish xenotransplant model was assessed (**Fig. 5**; Supplementary Fig. S6). In agreement with our above results, 72 hours of cetuximab exposure had no effect on apoptosis and tumor size of CACO-2 shControl tumors (**Fig. 5A**, **B**, **C–C'**, **D–D'**, **F**, and **G**). In contrast, combination of cetuximab with SHP099 showed a significant induction of cell death by apoptosis (∼2.25-fold increase in apoptosis $^{****}P < 0.0001$) followed by a reduction of about 27% of the tumor size ($^{**}P = 0.0096$; **Fig. 5B**, **C–C'**, **E–E'**, **F**, and **G**). Importantly, SHP099 treatment alone had no effect on apoptosis and tumor size of the same xenotransplanted colorectal cancer cells (Supplementary Fig. S6A and S6B–B', S6C–C', S6D, and S6E).

Moreover, combined treatment of cetuximab and SHP099 did not affect tumor size of CACO-2 shPLCG1 tumors when compared with cetuximab alone (P = ns; Supplementary Fig. S6G, H, I, J, and K), validating the benefit of the cotreatment only for tumors expressing high levels of PLCγ1.

Similarly, cetuximab-resistant SW48-PLCγ1 tumors showed a 50% decrease on tumor size and ∼5-fold increase of cell dead by apoptosis when SHP099 was added to cetuximab ($^{****}P < 0.0001$, **Fig. 5H**, **I–I'**, **J–J'**, **K–K'**, **L**, and **M**). However, SW48 sensitive tumors expressing lower levels of PLCγ1 did not show significant differences in tumor size when SHP099 was used in combination with cetuximab (P = ns; Supplementary Fig. S6M, N, O, P, and Q).

These results suggest that cetuximab and SHP099 treatment has an antitumor effect on resistant colorectal cancer cells such as CACO-2, but also on sensitive cells that became resistant purely by overexpression of PLCγ1 (SW48-PLCγ1), supporting the relevance of PLCγ1 expression in cetuximab+SHP099 treatment responses.

Finally, analysis of the metastatic potential showed that combined treatment can reduce in about 50%–60% metastases formation of both CACO-2 and SW48-PLCγ1 cetuximab-treated tumors ($^{*}P = 0.0219$ and 0.0127, respectively, **Fig. 5O** and **P**), overcoming PLCγ1-mediated resistance to cetuximab. Of note, SHP099 treatment alone did not reduce metastasis formation, nor added a significant benefit to cetuximab in CACO-2 shPLCG1 or SW48 cells expressing low levels of PLCγ1 (P = ns; Supplementary Fig. S6F, S6L and S6R). Yet, a slight reduction of metastasis formation was seen on CACO-2 shPLCG1 and SW48 cell lines when SHP099 was added to cetuximab which can be justified by the fact that both cell lines still express low levels of PLCγ1. Taken together, these results demonstrate a potential advantage of combinatorial therapy (cetuximab plus SHP2 inhibitor) in *RAS* WT patients with mCRC harboring PLCγ1-expressing tumors.

Discussion

Introduction of cetuximab in clinical practice has increased the median PFS of *RAS* WT patients with mCRC by 3.5 months (9). However, several resistance mechanisms to this drug have been reported (8–11, 42), underlining the need of new biomarkers that can better assist clinicians in the identification of responder patients, as well as the discovery of new therapeutic approaches to overcome resistance.

Our work reveals that levels of PLCγ1 expression can predict cetuximab responses in *RAS* WT colorectal cancer cell lines, zebrafish xenograft models, and primary tumor samples from patients with mCRC. Although cetuximab is administered in the metastatic setting, primary tumors are routinely used to assess patients' sensitivity to therapies, due to tissue availability. In this work, we demonstrated that levels of PLCγ1 expression remain significantly unchanged between primary colorectal cancer samples and metastases, making the primary sample a useful tool in assessing metastatic response. Therefore, median PFS for patients expressing low levels of PLCγ1 in primary samples was 7.1 months compared with 5.5 months for patients expressing high levels of this protein (log-rank $^{*}P = 0.0181$; HR, 0.6186; 95% CI, 0.3926–0.9012). Importantly, both groups of PLCγ1-expression patients were balanced for prognostic markers such as tumor location, age, *BRAF* mutations, as well as lines of cetuximab therapy and chemotherapy regimens undertaken (Supplementary Table S1). Although cetuximab is administered in combination with chemotherapy-based regimens in patients with mCRC, the predictive value of PLCγ1 expression seems specific for cetuximab responses, as supported by our *in vitro* and *in vivo* data where cetuximab was used as a single agent. Therefore, our results indicate that PLCγ1 expression in primary colorectal cancer samples is a strong independent biomarker that can reliably identify patients at increased risk of progression under cetuximab therapy.

Mechanistically, we found that, under cetuximab treatments, PLCγ1 can sustain EGFR downstream signaling regardless of EGFR levels. Accordingly, early clinical studies failed to correlate EGFR expression levels with clinical responses to EGFR inhibitor therapy (43). Furthermore, Chung and colleagues showed that several patients with CRC exhibited a major ORR to cetuximab despite the absence of measurable EGFR (by IHC; ref. 44). Although showing low levels of EGFR expression, CACO-2–resistant cell lines became 20% to 35% more sensitive to cetuximab in *in vitro* and *in vivo* models, when PLCγ1 expression was knockdown (**Figs. 1** and **2**). Similarly, SW48 cells became 20% and 40% more resistant to cetuximab when PLCγ1 was overexpressed (**Fig. 1**; Supplementary Fig. S2). Importantly, PLCγ1-induced resistance to cetuximab seems to be similar to the activation of other EGFR downstream pathways, such as PI3K whose activation was shown to induce 25% of resistance to cetuximab *in vitro* (34). Furthermore, PLCγ1 expression was associated with 60% to 75% increase on metastasis formation upon cetuximab treatment in the zebrafish xenotransplant model (**Fig. 2K**; Supplementary Fig. S2L). These results indicate that, in response to cetuximab treatment, PLCγ1 contributes, not only to tumor growth, but especially to metastasis development, in agreement with its reported crucial role in cancer cell migration and invasion (17, 45).

Taken together, our results support the previous findings that EGFR levels are not sufficient to predict cetuximab responses; instead levels of activation of downstream effectors, such as PLCγ1, reliably correlate

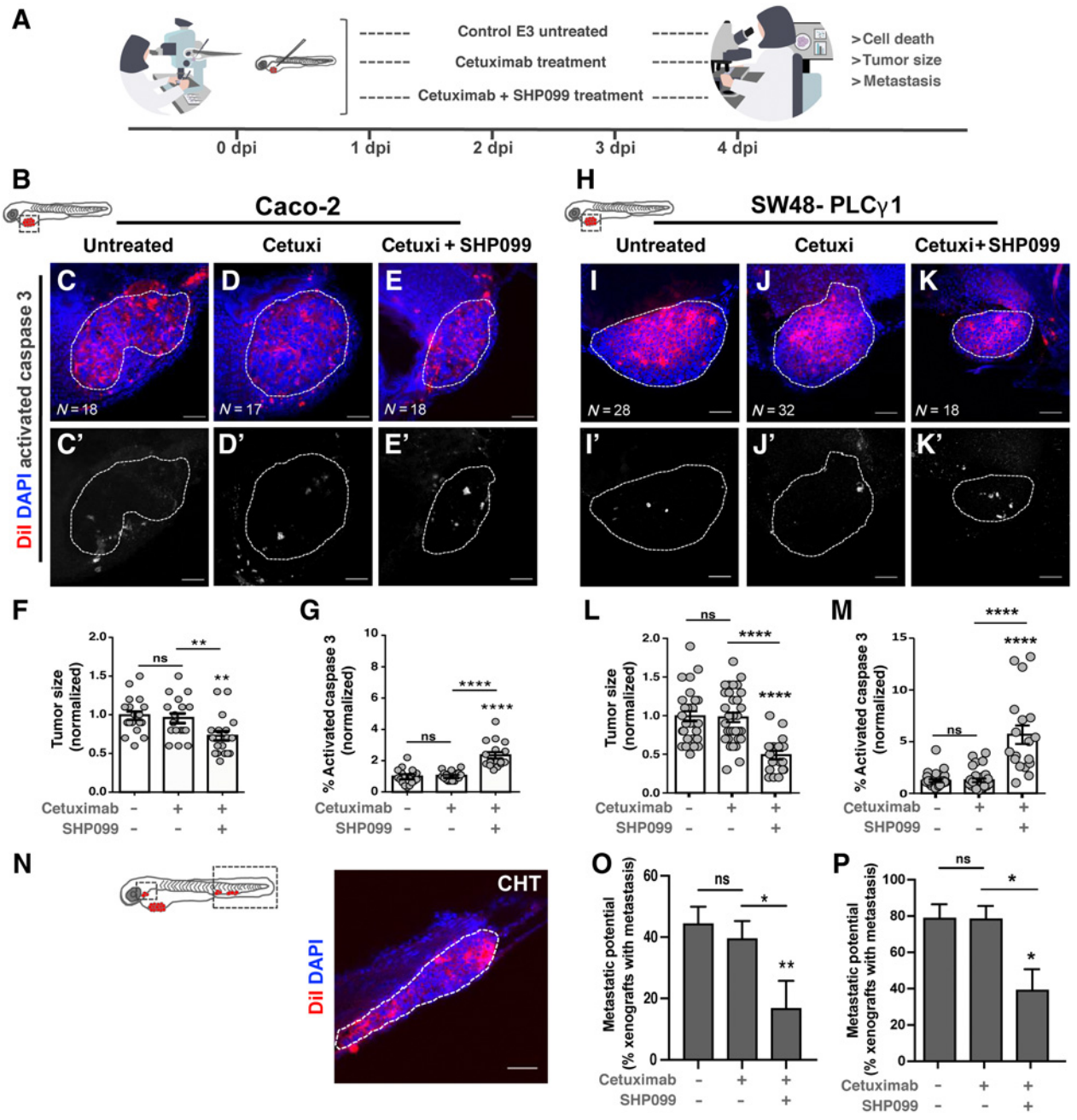

Figure 5.

Zebrafish xenotransplant model of CACO-2 shControl and SW48-PLCγ1 cells treated with cetuximab and SHP099. **A,** Cetuximab-resistant CACO-2 shControl and SW48-PLCγ1 were fluorescently lableled with DiI (red) and injected into the PVS of 2 dpf *nacre/casper* zebrafish larvae. Zebrafish xenografts were treated *in vivo* with cetuximab and SHP099 and compared with untreated controls regarding tumor size, cell death, and metastasis. **B–E',** At 4 dpi, zebrafish CACO-2 xenografts were imaged on PVS and over the zebrafish body by confocal microscopy. **F,** Analysis of CACO-2 tumor size (shControl vs. shControl cetuximab + SHP099, $^{**}P = 0.0017$; shControl cetuximab vs. shControl cetuximab + SHP099, $^{**}P = 0.0096$). **G,** Analysis of CACO-2 tumors activated caspase 3 (apoptosis; shControl vs. shControl cetuximab + SHP099, $^{****}P < 0.0001$; shControl cetuximab vs. shControl cetuximab + SHP099, $^{****}P < 0.0001$). **H–K',** At 4 dpi, zebrafish SW48–PLCγ1 xenografts were imaged on PVS and over the zebrafish body by confocal microscopy. **L,** Analysis of SW48–PLCγ1 tumor size (SW48–PLCγ1 vs. SW48–PLCγ1 cetuximab + SHP099, $^{****}P < 0.0001$; SW48–PLCγ1 cetuximab vs. SW48–PLCγ1 cetuximab + SHP099, $^{****}P < 0.0001$). **M,** Analysis of SW48–PLCγ1 tumors activated caspase 3 (apoptosis; SW48–PLCγ1 vs. SW48–PLCγ1 cetuximab + SHP099, $^{****}P < 0.0001$; SW48–PLCγ1 cetuximab vs. SW48–PLCγ1 cetuximab + SHP099, $^{****}P < 0.0001$). **N,** Representative image of micrometastasis in CHT. **O,** Analysis of CACO-2 metastasis (shControl cetuximab versus shControl cetuximab + SHP099, $^{*}P = 0.0219$; shControl versus shPLCγ1 cetuximab + SHP099, $^{**}P = 0{,}0046$). **P,** Analysis of SW48–PLCγ1 metastasis (SW48–PLCγ1 cetuximab vs. SW48–PLCγ1 cetuximab + SHP099, $^{*}P = 0.0127$; SW48–PLCγ1 vs. SW48–PLCγ1 cetuximab + SHP099, $^{*}P = 0.0116$). The outcomes are expressed as AVG ± SEM (ns > 0.05; *, $P \le 0.05$; **, $P \le 0.01$; ***, $P \le 0.001$; ****, $P \le 0.0001$). Scale bars = 50 μm.

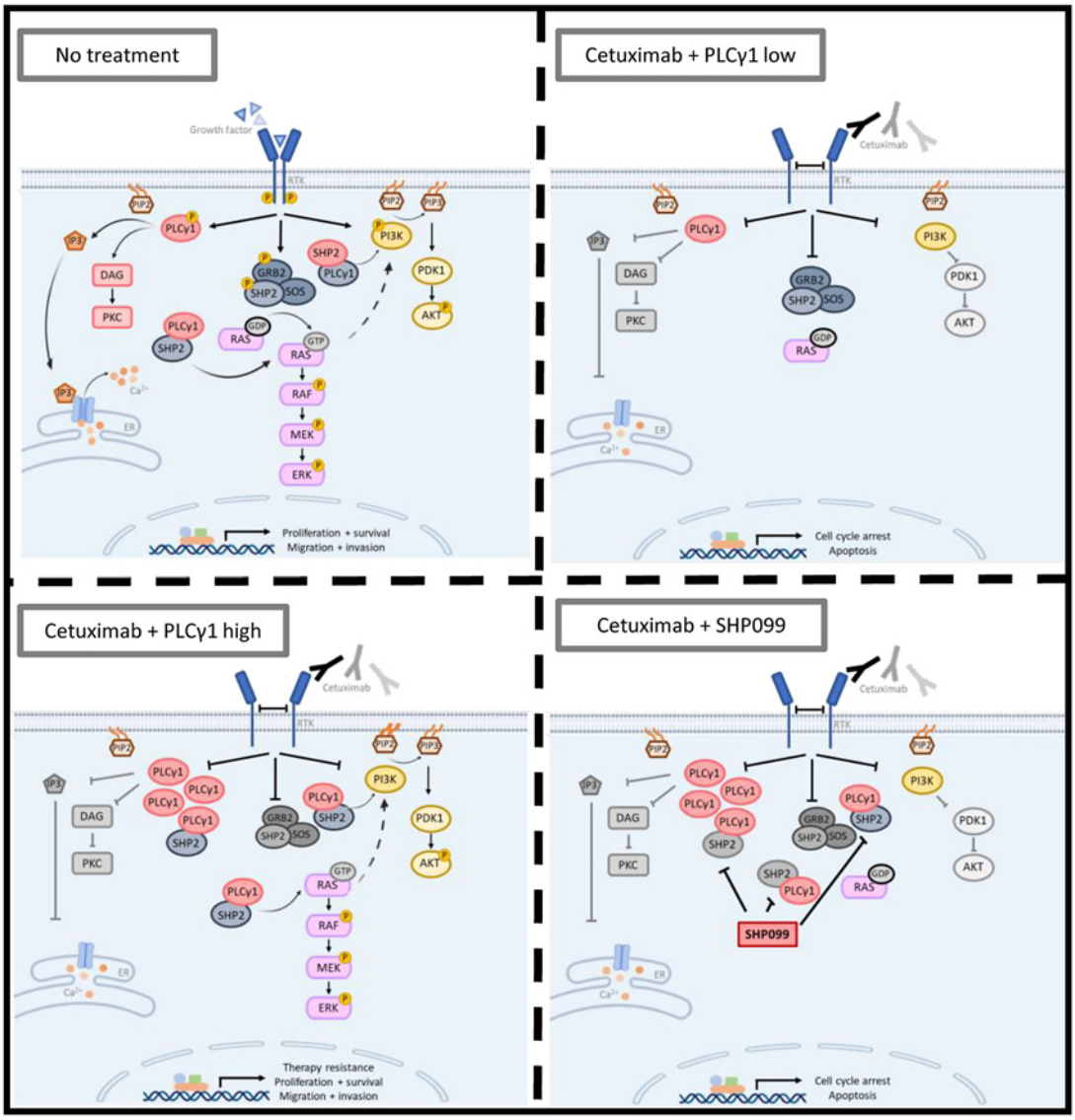

Figure 6.

PLCγ1-dependent mechanism of cetuximab resistance. Representative mechanism of cetuximab resistance dependent on PLCγ1 expression levels, based on findings described above. In colorectal cancer cells, binding of PLCγ1 to SHP2 is expected to transduce intracellular signs downstream of EGFR in parallel to ERK and AKT canonic signaling. When cancer cells are treated with anti-EGFR therapies, EGFR downstream signaling is inhibited. However, PLCγ1–SHP2 axis is able to sustain downstream signaling, when levels of PLCγ1 are high, inducing cetuximab resistance. Combination of EGFR-targeted therapy with anti-SHP2 inhibitors benefits colorectal cancer tumors with PLCγ1 overexpression.

with signaling transduction and responses, and should be taken into clinical consideration.

Surprisingly, we found that the role of PLCγ1 in this process is independent of its lipase activity. Very few reports have shown a role of PLCγ1 in EGFR mitogenic signaling independent of its catalytic activity. For instance, Pei and colleagues have demonstrated that PLCγ1 can signal downstream of EGFR through binding to the adaptor growth factor receptor-bound protein 2 (GRB2) and son of sevenless guanine nucleotide exchange factor (SOS), in a mechanism independent of PLCγ1 Y783 phosphorylation (46). Xie and colleagues have identified PLCγ1 SH3 domain as essential for EGF-induced squamous cell carcinoma (SCC) growth (47). In our work, we found that nSH2-cSH2 domains are essential for PLCγ1-induced resistance to cetuximab through binding to SHP2. In this context, PLCγ1 seems to bind to SHP2 independently of its phosphorylated Y783 residue, and confer proliferative and anti-apoptotic advantage to colorectal cancer cells when treated with anti-EGFR mAbs. Importantly, SHP2 has been shown involved in the regulation of the same cellular processes through activation of the RAS/ERK cascade (48), activation of PI3K/AKT pathway (49), and inhibition of p53-mediated apoptosis (50). Therefore, we propose a model where PLCγ1, when highly abundant, interacts with SHP2, induces its activation and subsequent signaling (**Fig. 6**). Despite our evidence of PLCγ1 and SHP2 interaction, some questions remain to be elucidated, such as: how the binding occurs; whether it is a direct or indirect binding; how is it regulated; and which SHP2 domains are involved. Nevertheless, upon cetuximab

treatment, where EGFR signaling is inhibited, PLCγ1–SHP2 binding is sufficient to maintain, at least in part, the intracellular cascade (**Fig. 6**). On the other hand, when PLCγ1 levels are low, PLCγ1–SHP2 binding is absent/minimal and cetuximab induces an effective downregulation of intracellular signaling cascades (**Fig. 6**).

In agreement, combined treatments of cetuximab with a SHP2 inhibitor show antitumor effects in PLCγ1-dependent cetuximab-resistant cancer cells (**Figs. 4** and **5**; Supplementary Fig. S6). SHP2 inhibitors (such as TNO155) are presently in clinical trials, both alone or in combination with inhibitors of activated EGFR (nazartinib), for the treatment of solid tumors (ClinicalTrials.gov ID: NCT03114319). Our results suggest that inhibition of SHP2 and EGFR WT may also benefit patients with colorectal cancer harboring high levels of PLCγ1.

Overall, this work contributes to a better understanding of the mechanisms of resistance to anti-EGFR therapies, uncovering a novel biomarker predictive of response to cetuximab and a new therapeutic strategy to revert resistance in *RAS* WT mCRC patients.

Authors' Disclosures

P. Borralho reports grants from Roche and Novartis, as well as personal fees from Bayer and AstraZeneca outside the submitted work. D. Machado reports personal fees from Amgen and Merck outside the submitted work. H. Mansinho reports grants from AstraZeneca; nonfinancial support from AstraZeneca; and personal fees from Roche, Pfizer, Pierre Fabre, Incyte, BMS, Novartis, Amgen, Servier, Merck Serono, and Grunenthal outside the submitted work. A. Mansinho reports personal fees and nonfinancial support from Merck-Serono during the conduct of the study, as well as personal fees and nonfinancial support from Amgen, Astellas, Bayer, Bristol Myers Squibb, Janssen, Merck Sharp & Dohme, Novartis, Vifor Pharma, Pfizer, Pierre Fabre, Roche, and Servier outside the submitted work. L. Costa reports grants from Merck-Serono during the conduct of the study. M. Martins reports grants from Liga Portuguesa Contra o Cancro/Terry Fox and Merck-Serono during the conduct of the study. No disclosures were reported by the other authors.

Authors' Contributions

R. Cruz-Duarte: Investigation, methodology. **C. Rebelo de Almeida:** Investigation, methodology. **M. Negrão:** Investigation, methodology. **A. Fernandes:** Investigation, methodology. **P. Borralho:** Investigation, methodology. **D. Sobral:** Software, investigation. **L.M. Gallego-Paez:** Software, investigation. **D. Machado:** Investigation. **J. Gramaça:** Investigation. **J. Vílchez:** Investigation. **A.T. Xavier:** Investigation. **M. Godinho Ferreira:** Funding acquisition. **A.R. Miranda:** Investigation. **H. Mansinho:** Investigation. **M.J. Brito:** Investigation. **T.R. Pacheco:** Conceptualization. **C. Abreu:** Investigation. **A. Lucia-Costa:** Investigation. **A. Mansinho:** Investigation. **R. Fior:** Supervision, funding acquisition, investigation, methodology, writing–review and editing. **L. Costa:** Conceptualization, resources, supervision, funding acquisition, writing–review and editing. **M. Martins:** Conceptualization, supervision, funding acquisition, investigation, methodology, writing–original draft, project administration.

Acknowledgments

We acknowledge the help of Carla Sousa and Genomed for assessing *RAS* mutations on tumor samples, the help of Dr. Vasco Rodrigues, and Dr. Rui Marques for their contribution at the Hospital Santa Maria Pharmacy and Champalimaud Fish Platform (C. Certal and J. Monteiro) for excellent animal care. We thank Tom Bunney and Matilda Katan for helpful advice on this project and contribution with PLCγ1 plasmids. The authors thank Champalimaud Foundation and M. Godinho Ferreira for the initial support of this project. M. Martins' research was supported by Liga Portuguesa Contra o Cancro (LPCC): Terry Fox Fundation; Investigador FCT-Fundação para a Ciência e Technologia (IF/00409/2014) and IMM Bridge grant; RC-D research was supported by Fundação para a Ciência e Technologia (SFRH/BD/139138/2018). A. Fernandes was supported by LPCC-IMM BIOBANK; R. Fior was supported by Champalimaud Foundation and L. Costa was supported by Merck Serono.

The costs of publication of this article were defrayed in part by the payment of page charges. This article must therefore be hereby marked *advertisement* in accordance with 18 U.S.C. Section 1734 solely to indicate this fact.

Received May 31, 2021; revised November 14, 2021; accepted December 27, 2021; published first January 3, 2022.

References

1. Bray F, Ferlay J, Soerjomataram I, Siegel RL, Torre LA, Jemal A. Global cancer statistics 2018: GLOBOCAN estimates of incidence and mortality worldwide for 36 cancers in 185 countries. CA Cancer J Clin 2018;68:394–424.
2. Spano JP, Lagorce C, Atlan D, Milano G, Domont J, Benamouzig R, et al. Impact of EGFR expression on colorectal cancer patient prognosis and survival. Ann Oncol 2005;16:102–8.
3. Tabernero J, Van Cutsem E, Díaz-Rubio E, Cervantes A, Humblet Y, André T, et al. Phase II trial of cetuximab in combination with fluorouracil, leucovorin, and oxaliplatin in the first-line treatment of metastatic colorectal cancer. J Clin Oncol 2007;25:5225–32.
4. Douillard JY, Siena S, Cassidy J, Tabernero J, Burkes R, Barugel M, et al. Randomized, phase III trial of panitumumab with infusional fluorouracil, leucovorin, and oxaliplatin (FOLFOX4) versus FOLFOX4 alone as first-line treatment in patients with previously untreated metastatic colorectal cancer: the PRIME study. J Clin Oncol 2010;28:4697–705.
5. Ciardiello F, Tortora G. EGFR antagonists in cancer treatment. N Engl J Med 2008;358:1160–74.
6. Yang X, Zhang X, Mortenson ED, Radkevich-Brown O, Wang Y, Fu YX. Cetuximab-mediated tumor regression depends on innate and adaptive immune responses. Mol Ther 2013;21:91–100.
7. Wang L, Wei Y, Fang W, Lu C, Chen J, Cui G, et al. Cetuximab enhanced the cytotoxic activity of immune cells during treatment of colorectal cancer. Cell Physiol Biochem 2017;44:1038–50.
8. Sorich MJ, Wiese MD, Rowland A, Kichenadasse G, McKinnon RA, Karapetis CS. Extended *RAS* mutations and anti-EGFR monoclonal antibody survival benefit in metastatic colorectal cancer: a meta-analysis of randomized, controlled trials. Ann Oncol 2015;26:13–21.
9. Van Cutsem E, Lang I, Folprecht G, Nowacki M, Barone C, Shchepotin I, et al. Cetuximab plus FOLFIRI: final data from the CRYSTAL study on the association of KRAS and BRAF biomarker status with treatment outcome. J Clin Oncol 2010;28:3570.
10. De Roock W, Claes B, Bernasconi D, De Schutter J, Biesmans B, Fountzilas G, et al. Effects of KRAS, BRAF, NRAS, and PIK3CA mutations on the efficacy of cetuximab plus chemotherapy in chemotherapy-refractory metastatic colorectal cancer: a retrospective consortium analysis. Lancet Oncol 2010;11:753–62.
11. Karapetis CS, Jonker D, Daneshmand M, Hanson JE, O'Callaghan CJ, Marginean C, et al. PIK3CA, BRAF, and PTEN status and benefit from cetuximab in the treatment of advanced colorectal cancer-results from NCIC CTG/AGITG CO.17. Clin Cancer Res 2014;20:744–53.
12. Ji QS, Ermini S, Baulida J, Sun FL, Carpenter G. Epidermal growth factor signaling and mitogenesis in Plcg1 null mouse embryonic fibroblasts. Mol Biol Cell 1998;9:749–57.
13. Ji QS, Winnier GE, Niswender KD, Horstman D, Wisdom R, Magnuson MA, et al. Essential role of the tyrosine kinase substrate phospholipase C-γ1 in mammalian growth and development. Proc Natl Acad Sci U S A 1997;94:2999–3003.
14. Meisenhelder J, Suh PG, Rhee SG, Hunter T. Phospholipase C- γ1 is a substrate for the PDGF and EGF receptor protein-tyrosine kinases in vivo and in vitro. Cell 1989;57:1109–22.
15. Bunney TD, Esposito D, Mas-Droux C, Lamber E, Baxendale RW, Martins M, et al. Structural and functional integration of the PLCγ interaction domains critical for regulatory mechanisms and signaling deregulation. Structure 2012;20:2062–75.
16. Xie Z, Chen Y, Liao EY, Jiang Y, Liu FY, Pennypacker SD. Phospholipase C-γ1 is required for the epidermal growth factor receptor-induced squamous cell carcinoma cell mitogenesis. Biochem Biophys Res Commun 2010;25:296–300.
17. Jones NP, Peak J, Brader S, Eccles SA, Katan M. PLCγ1 is essential for early events in integrin signalling required for cell motility. J Cell Sci 2005;118:2695–706.

18. Thomas SM, Coppelli FM, Wells A, Gooding WE, Song J, Kassis J, et al. Epidermal growth factor receptor-stimulated activation of phospholipase Cγ-1 promotes invasion of head and neck squamous cell carcinoma. Cancer Res 2003;63:5629–35.
19. Behjati S, Tarpey PS, Sheldon H, Martincorena I, Van Loo P, Gundem G, et al. Recurrent PTPRB and PLCG1 mutations in angiosarcoma. Nat Genet 2014;46:376–9.
20. Vaqué J, Gómez-López G, Monsálvez V. PLCG1 mutations in cutaneous T-cell lymphomas. Blood 2014;123:2034–44.
21. Noh DY, Lee YH, Kim SS, Kim YI, Ryu SH, Suh PG, et al. Elevated content of phospholipase C-gamma 1 in colorectal cancer tissues. Cancer 1994;73:36–41.
22. Prenen H, Smeets D, Mazzone M, Lambrechts D, Sagaert X, Sciot R. Phospholipase C gamma 1 (PLCG1) R707Q mutation is counterselected under targeted therapy in a patient with hepatic angiosarcoma. Oncotarget 2015;6:36418–25.
23. Woyach JA, Furman RR, Liu TM, Ozer HG, Zapatka M, Ruppert AS, et al. Resistance mechanisms for the Bruton's tyrosine kinase inhibitor ibrutinib. N Engl J Med 2014;370:2286–94.
24. Robinson MD, McCarthy DJ, Smyth GK. edgeR: a Bioconductor package for differential expression analysis of digital gene expression data. Bioinformatics 2009;26:139–40.
25. Khan MS, Dodson AR, Heatley MK. Ki-67, oestrogen receptor, and progesterone receptor proteins in the human rete ovarii and in endometriosis. J Clin Pathol 1999;52:517–20.
26. Fior R, Póvoa V, Mendes RV, Carvalho T, Gomes A, Figueiredo N, et al. Single-cell functional and chemosensitive profiling of combinatorial colorectal therapy in zebrafish xenografts. Proc Natl Acad Sci U S A 2017;114:E8234–43.
27. Muzny DM, Bainbridge MN, Chang K, Dinh HH, Drummond JA, Fowler G, et al. Comprehensive molecular characterization of human colon and rectal cancer. Nature 2012;487:330–7.
28. Lim B, Mun J, Kim JH, Kim CW, Roh SA, Cho DH, et al. Genome-wide mutation profiles of colorectal tumors and associated liver metastases at the exome and transcriptome levels. Oncotarget 2015;6:22179–90.
29. Picco G, Chen ED, Alonso LG, Behan FM, Gonçalves E, Bignell G, et al. Functional linkage of gene fusions to cancer cell fitness assessed by pharmacological and CRISPR-Cas9 screening. Nat Commun 2019;10:2198.
30. Stransky N, Ghandi M, Kryukov GV, Garraway LA, Lehár J, Liu M, et al. Pharmacogenomic agreement between two cancer cell line data sets. Nature 2015;528:84–7.
31. Iorio F, Knijnenburg TA, Vis DJ, Bignell GR, Menden MP, Schubert M, et al. A landscape of pharmacogenomic interactions in cancer. Cell. 2016;166:740–54.
32. Ghandi M, Huang FW, Jané-Valbuena J, Kryukov GV, Lo CC, McDonald ER, et al. Next-generation characterization of the Cancer Cell Line Encyclopedia. Nature 2019;569:503–8.
33. Barretina J, Caponigro G, Stransky N, Venkatesan K, Margolin AA, Kim S, et al. The cancer cell line encyclopedia enables predictive modelling of anticancer drug sensitivity. Nature 2012;483:603–7.
34. Ashraf SQ, Nicholls AM, Wilding JL, Ntouroupi TG, Mortensen NJ, Bodmer WF. Direct and immune mediated antibody targeting of ERBB receptors in a colorectal cancer cell-line panel. Proc Natl Acad Sci U S A 2012;109:21046–51.
35. Jhawer M, Goel S, Wilson AJ, Montagna C, Ling YH, Byun DS, et al. PIK3CA mutation/PTEN expression status predicts response of colon cancer cells to the epidermal growth factor receptor inhibitor cetuximab. Cancer Res 2008;68:1953–61.
36. Fazio M, Ablain J, Chuan Y, Langenau DM, Zon LI. Zebrafish patient avatars in cancer biology and precision cancer therapy. Nat Rev Cancer 2020;20:263–73.
37. Zhang Q, Yu C, Peng S, Xu H, Wright E, Zhang X, et al. Autocrine VEGF signaling promotes proliferation of neoplastic Barrett's epithelial cells through a PLC-dependent pathway. Gastroenterology 2014;146:461–72.
38. Shin SY, Choi HY, Ahn BH, Min DS, Son SW, Lee YH. Phospholipase Cγ1 stimulates transcriptional activation of the matrix metalloproteinase-3 gene via the protein kinase C/Raf/ERK cascade. Biochem Biophys Res Commun 2007;353:611–6.
39. Karapetis CS, Khambata-Ford S, Jonker DJ, O'Callaghan CJ, Tu D, Tebbutt NC, et al. K-ras mutations and benefit from cetuximab in advanced colorectal cancer. N Engl J Med 2008;359:1757–65.
40. Pawson T. Specificity in signal transduction: From phosphotyrosine-SH2 domain interactions to complex cellular systems. Cell 2004;116:191–203.
41. Agazie YM, Hayman MJ. Molecular mechanism for a role of SHP2 in epidermal growth factor receptor signaling. Mol Cell Biol 2003;23:7875–86.
42. Martins M, Mansinho A, Cruz-Duarte R, Martins SL, Costa L. Anti-EGFR therapy to treat metastatic colorectal cancer: Not for all. Adv Exp Med Biol 2018;1110:113–31.
43. Kim TW. EGFR status is not a reliable biomarker to select patients suitable for cetuximab-based therapy. Clin Colorectal Cancer 2014;13:3–4.
44. Chung KY, Shia J, Kemeny NE, Shah M, Schwartz GK, Tse A, et al. Cetuximab shows activity in colorectal cancer patients with tumors that do not express the epidermal growth factor receptor by immunohistochemistry. J Clin Oncol 2005;23:1803–10.
45. Kassis J, Lauffenburger DA, Turner T, Wells A. Tumor invasion as dysregulated cell motility. Semin Cancer Biol 2001;11:105–17.
46. Pei Z, Maloney JA, Yang L, Williamson JR. A new function for phospholipase C-γ1: coupling to the adaptor protein GRB2. Arch Biochem Biophys 1997;345:103–10.
47. Xie Z, Chen Y, Pennypacker SD, Zhou Z, Peng D. The SH3 domain, but not the catalytic domain, is required for phospholipase C-γ1 to mediate epidermal growth factor-induced mitogenesis. Biochem Biophys Res Commun 2010;398:719–22.
48. Rehman AU, Rahman MU, Khan MT, Saud S, Liu H, Song D, et al. The landscape of protein tyrosine phosphatase (Shp2) and cancer. Curr Pharm Des 2018;24:3767–77.
49. Zito CI, Kontaridis MI, Fornaro M, Feng GS, Bennett AM. SHP-2 regulates the phosphatidylinositide 3′-Kinase/Akt pathway and suppresses caspase 3-mediated apoptosis. J Cell Physiol 2004;199:227–36.
50. Stewart RA, Sanda T, Widlund HR, Zhu S, Swanson KD, Hurley AD, et al. Phosphatase-dependent and -independent functions of Shp2 in neural crest cells underlie LEOPARD syndrome pathogenesis. Dev Cell 2010;18:750–62.